International Journal of Electronics

ISSN: 0020-7217 (Print) 1362-3060 (Online) Journal homepage: https://www.tandfonline.com/loi/tetn20

Design and simulation of a tactile display based on a CMUT array

Vasilios G. Chouvardas , Miltiadis K. Hatalis & Amalia N. Miliou

To cite this article: Vasilios G. Chouvardas , Miltiadis K. Hatalis & Amalia N. Miliou (2012) Design and simulation of a tactile display based on a CMUT array, International Journal of Electronics, 99:10, 1351-1363, DOI: 10.1080/00207217.2012.669714

To link to this article: https://doi.org/10.1080/00207217.2012.669714

International Journal of Electronics
Vol. 99, No. 10, October 2012, 1351–1363

Taylor & Francis
Taylor & Francis Group

Design and simulation of a tactile display based on a CMUT array

Vasilios G. Chouvardas[a], Miltiadis K. Hatalis[b] and Amalia N. Miliou[a]*

[a]*Informatics Department, Aristotle University of Thessaloniki, P.O. Box 114, 541 24 Thessaloniki, Greece;* [b]*Department of Electrical and Computer Engineering, Lehigh University, Bethlehem, PA 18015, USA*

(*Received 14 July 2011; final version received 5 February 2012*)

In this article, we present the design of a tactile display based on a CMUT-phased array. The array implements a 'pixel' of the display and is used to focus airborne ultrasound energy on the skin surface. The pressure field, generated by the focused ultrasound waves, is used to excite the mechanoreceptors under the skin and transmit tactile information. The results of Finite Element Analysis (FEA) of the Capacitive Micromachined Ultrasonic Transducer (CMUT) and the CMUT-phased array for ultrasound emission are presented. The 3D models of the device and the array were developed using a commercial FEA package. Modelling and simulations were performed using the parameters from the *POLYMUMPS* surface micromachining technology from *MEMSCAP*. During the analysis of the phased array, several parameters were studied in order to determine their importance in the design of the tactile display. The output of the array is compared with the acoustic intensity thresholds in order to prove the feasibility of the design. Taking into account the density of the mechanoreceptors in the skin, we conclude that there should be at least one receptor under the excitation area formed on the skin.

Keywords: tactile displays; tactile communication; tactation; tangible interface; MEMS; CMUT; ultrasonic; phased array

1. Introduction

Tactile displays are human–computer interfaces, that utilise the sense of tactation and convey information from the machine to humans. An extended review of skin physiology and tactile display technologies and applications is described by Chouvardas, Miliou, and Hatalis (2008). Tactile displays utilise one of the following skin modalities: (i) vibration, (ii) pressure and stroking, (iii) skin stretch and (iv) texture stroking and fluttering. Skin modalities are the channels through which energy is transmitted to the skin and excites the mechanoreceptors that are responsible for the sense of tactation. Ultrasound tactile displays are based on the vibration modality, through which the Pacinian corpuscles are excited.

Ultrasonic transducers have been widely used in the areas of Non-destructive-esting (NDT) (Greve and Openheim 2003) and flaw detection (Jain, Greve, and Openheim 2003), medical imaging (Wygant et al. 2005), therapy (tissue ablation) (Saleh and Smith 2004), tactile displays (Iwamoto, Maeda, and Shinoda 2001; Hoshi, Takahashi, and Shinoda 2010), range finding, etc. Commercial transducers are often made of quartz or

*Corresponding author. Email: amiliou@csd.auth.gr

ISSN 0020–7217 print/ISSN 1362–3060 online

http://dx.doi.org/10.1080/00207217.2012.669714
http://www.tandfonline.com

piezo-ceramics (like lead zirconate titanate (PZT), lithium niobate, zinc oxide, etc.) or ferroelectrics (giant electrostriction devices).

The motivation behind this work is the design of an integrated tactile display that will use airborne ultrasound as a means to excite the skin mechanoreceptors and transmit tactile information to the skin. Therefore, we propose that the source of ultrasound energy in a tactile display can be a CMUT-phased array. The idea of using such a device for tactile displays is based on previous work conducted by Iwamoto et al. (2001). More specifically, Iwamoto et al. used off-the-shelf PZT transducer arrays as an ultrasound source and constructed an efficient, high-output yet bulky tactile display.

In recent years, there has been a significant progress in modelling, design and fabrication of CMUTs (Kazys, Jakevicious, and Mazeika 1998; Bozkurt 2003) and CMUT arrays (Teston, Certon, Patat, and Felix 2005). The device can be fabricated using mature MEMS micro-machining technologies. Compared to piezo-electrics, CMUTs are better in terms of cost, flexibility and repeatability. Also, since CMUT fabrication can be made with CMOS MEMS techniques, we can achieve monolithic integration of the transducers along with the necessary logic and drive circuitry. The CMUT can be used either as a sensor or an actuator.

Section 2 of this article, discusses the idea of the use of CMUTs as ultrasound source for tactile displays along with the transducer model and precise simulation results on its behaviour. The array model is described and the simulation results are presented in Section 3. Concluding remarks on the tactile display design and simulation are discussed in Section 4.

2. Modelling and simulation of the CMUT transducer

The skin mechanoreceptors can be excited by: (i) pin arrays (Nakatani, Kajimoto, Kawakami, and Tachi 2005) (ii) ER fluids (Klein et al. 2005) and (iii) ultrasound. In order to ensure high resolution on the tactile display, we use high-frequency ultrasound. Focusing the output of a large number of transducers, arranged as a phased array, will produce high levels of pressure on the skin. Furthermore, it is important that the acoustic pressure at the focal point must exceed the excitation threshold for the operating frequency.

In order to design the tactile display, it is important to study the behaviour of the individual transducer and the array and also define the factors that affect their operation and performance. For this purpose, a model of the transducer and the array has been developed and their operation is studied extensively through simulation.

2.1. *Simulation environment*

For our simulations, we have used the *ANSYS* package, which proved suitable in terms of speed, flexibility, programming and memory usage. We developed custom code for the coupled physics environment and performed a large number of runs for static, harmonic, modal and transient analysis of the individual transducer as well as the transducer array. The simulation was performed on a HP DL385 dual *Opteron* 2.4 GHz server with 11GB of RAM and two Intel CORE 2 QUAD 2.4 GHZ–8 GB RAM and 2.83 GHZ–8 GB RAM PCs. Several disk configurations were used; the fastest being RAID0 stripped arrays.

2.2. *Transducer model*

A CMUT is a two-electrode system (Figure 1) where the two electrodes are plates. One plate is fully clamped while the other is only clamped at the edges, which allows for free movement or vibration. By applying an electric potential between the plates, the free plate is forced to move towards the clamped one. A time-varying sinusoidal voltage at the resonance frequency F_0 of the system, will force the free plate to oscillate with a maximum displacement. In the design shown in Figure 1, the material of the two electrodes is polysilicon. A 3D model of the transducer is shown in Figure 2. For modelling and simulation purposes, we use the material properties and the dimensions from the PolyMUMPS Design Manual[1] as shown in Tables 1 and 2, respectively. PolyMUMPS technology is a set of specifications for the design of MEMS using surface micromachining.

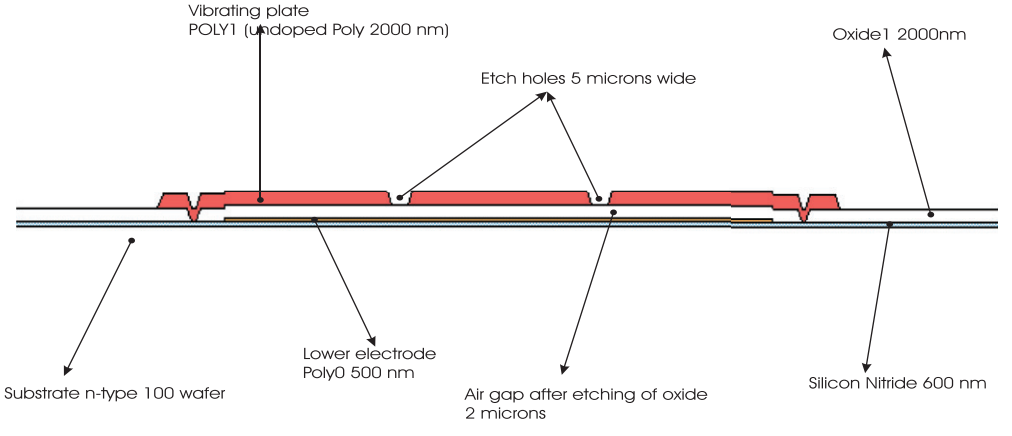

Figure 1. Transducer profile.

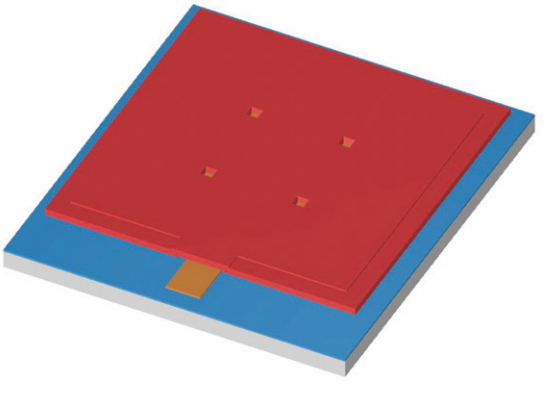

Figure 2. 3D model of the transducer.

Table 1. Material properties for the finite element model.

Component (material)	Plate (poly)	Air gap
Young's modulus (N/m^2)	158×10^9	
Density (Kg/m^3)	2320	–
Poisson ratio	0.22	–
Permivity ($F/\mu m$)	–	8854×10^{-16}

Table 2. Geometric constants for the transducer model.

Parameter	Plate thickness	Air gap (initial)	Plate edge or diameter
Dimension (μm)	2	2	50–600

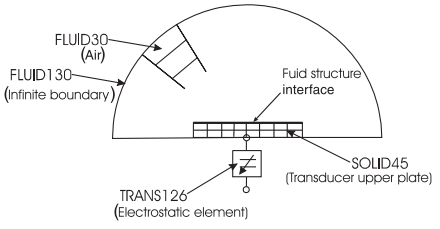

Figure 3. Transducer simulation model.

The basis of the CMUT array is a detailed model of a single CMUT device, which involves coupled physics and electrostatics-structural-fluid interactions, starting from the electrical excitation of the CMUT and ending in the propagation of sound waves and generation of a pressure field. The idea is that the solution of one physics domain is used as the initial condition for the next, in a cyclical manner. More specifically, during each simulation cycle:

(1) a voltage difference is applied between the transducer's plates;
(2) the applied voltage creates an electrostatic force between the plates;
(3) the free plate is forced to move and bend;
(4) the plate movement creates a pressure difference in the fluid;
(5) the pressure difference propagates as a sound wave.

The simulation model includes a system of equations, the elements and meshing and the proper solver. A graphical representation of the simulation model is shown in Figure 3.

2.2.1. *Model equations*

The plate displacement was calculated using a generalised form of Hooke's law. The plate vibration is described by Newton's second law, where the elastic forces are described by

Hooke's law (Equation (1)):

$$\rho h \frac{\partial^2 \omega'}{\partial t^2} - T\nabla^2 \omega' + D\nabla^4 \omega' = f(x', y', z') \tag{1}$$

The plate's deflection is denoted by ω, ρ is the material density, h is the plate thickness, $D = Eh^3/(12(1-N))$ is flexural rigidity, E is Young's modulus, N is the Poisson ratio and f is the load function created by the electrostatic force and the fluid–structure interaction. Equation (1) applies when the system vibrates in vacuum, i.e. no damping term is present. However, due to the presence of the fluid and the fluid–structure interface in our model, the necessary damping is added.

Propagation was modelled with the wave equation:

$$\frac{1}{c}\frac{\partial^2 P}{\partial t^2} - \nabla^2 P = 0 \tag{2}$$

where P is the fluid pressure, t is the time, $c = \sqrt{k/\rho_0}$ is the speed of sound in the fluid, ρ_0 is the fluid density and k is the bulk modulus of the fluid.

The energy transfer between the structure and fluid domains is realised by their coupling at the 'fluid–structure interface' (FSI) area and is modelled with linear constraint equations, that relate the nodes of the structure (transducer), with the elements of the fluid.

FEA was used to solve the system equations and to evaluate the resonance frequency, radiated pressure and membrane deflections. All the above are critical parameters, required to design and optimise CMUT for improved performance. The solution includes the harmonics, the vibration modes and the air pressure at the output of the transducer. The plate is assumed to vibrate in air, therefore, both the energy absorption from the air and damping had to be taken into account during the simulation process.

2.2.2. *Meshing*

The transducer plate, described in Figure 3, was meshed with the *Solid*45 element, which is commonly used for the 3D modelling of solid structures. The element is defined by eight nodes having three degrees of freedom at each node (translation in the nodal x, y, and z directions). Also, the elements exhibit plasticity, creep, swelling, stress stiffening, large deflection and large strain capabilities (ANSYS Documentation 2010).

The air gap and the lower electrode of the transducer were modelled with the *Trans*126 element, that converts energy from the electrostatic domain into the structural domain and vice versa. The element fully couples the electromechanical domains and is suitable for structural finite element analysis.

Additionally, the fluid (air) was meshed with *Fluid*30 element, which is used for modelling the fluid and FSI in fluid/structure interaction problems (Figure 3). At the edge of the fluid area we used *Fluid*130 elements, which are companion elements to *Fluid*30 and simulate the absorbing effects of a fluid domain, that extends to infinity beyond the boundary of the finite element domain. In this way, reflection of the sound wave at the boundary was avoided.

Although in the phased array under investigation, we used only rectangular transducers, in the harmonic analysis we have used both rectangular as well as circular plates in order to compare the results. Two different strategies have been followed for the meshing of the rectangular and circular plates. Mapped meshing and hexahedral elements were used for the rectangular transducer, while free meshing and tetrahedral element were

used for the circular. More specifically, we generated a triangular surface mesh at the top surface and we swept it towards the other surface. The construction of the mesh for circular transducer required an iterative process with several passes of local optimisation until an acceptable element size was met.

2.3. *Analysis*

In order to study the effect of DC bias voltage on the resonance frequency harmonic analysis, with and without prestress was performed. Furthermore, the acoustic pressure field in free air was calculated so as to have an estimate of the transducer output. The analysis was conducted using '*SPARSE*' direct equation solver, provided by *ANSYS* (ANSYS Documentation 2010), which is usually applicable for static, harmonic and transient analysis and it combines speed and robustness.

2.3.1. *Harmonic analysis*

Harmonic analysis was performed in order to determine the resonance frequency F_0. The upper electrode is the vibrating plate and was put at ground voltage while a voltage ranging from 30 to 100 V was applied to the lower electrode. Figure 4 shows the harmonic analysis for a 135 μm × 135 μm plate. As it is clear in Figure 4, F_0 is 1.533 MHz and also the displacement at the center of the plate at F_0 is 0.195 μm. High Q is directly observable (Q is 1000), and it can be altered, for a given plate thickness, by changing the plate dimensions.

Larger plates have lower stiffness and also lower resonance frequency. The results of the harmonic analysis for several plate sizes, in the case of rectangular and circular plates are presented in Figure 5(a) and (b), respectively. More specifically as shown in Figure 5(a) in the case of a rectangular plate, F_0 decreases as a function of s, where s is plate size. Furthermore, when circular plates are used F_0 exhibits a linear increase as a function of $1/(r^2)$, where r is the transducer radius (Figure 5(b)). Finally, a snapshot of the time domain analysis is shown in Figure 6 where the acoustic pressure field above the transducer is presented.

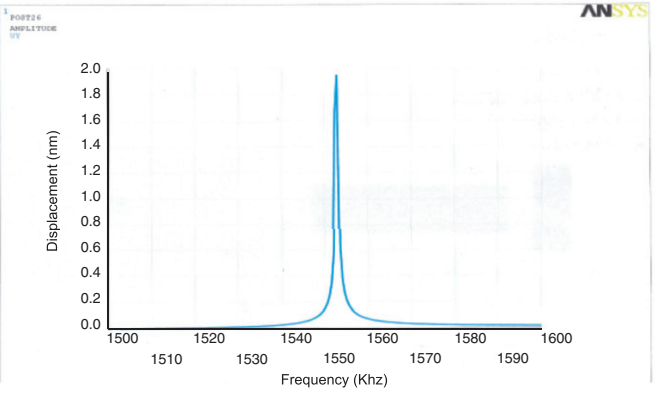

Figure 4. Harmonic analysis results of a 135 μm × 135 μm transducer.

2.3.2. *Harmonic analysis with prestress*

In an effort to determine the dependence of the resonant frequency of a prestressed device on the bias voltage, a DC bias voltage was applied on the electrodes. In the analysis the transducer was rectangular with $120\,\mu m \times 120\,\mu m$ plates. The simulation included two steps. First, a static analysis was performed in order for the plate to deform under the bias voltage. Secondly, an harmonic analysis was conducted and the results are shown in Figure 7. Fitting the experimental results, shown in black squares in Figure 7, revealed that the dependance of F_0 on the bias voltage has a polynomial decay and follows the expression $F_0(V) = 1937000 - V^2$.

3. Simulation of the array

The CMUT array is a 2D grid of transducers (Figure 8). For symmetry reasons, the array step was chosen equal in both directions. The focal point was at a distance above the center

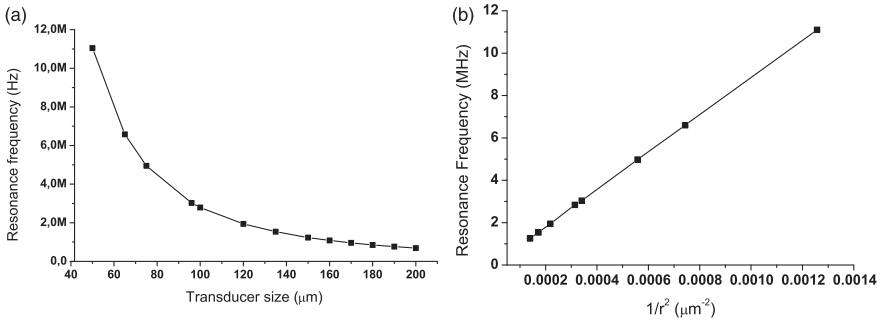

Figure 5. Simulation results for F_0. (a) F_0 versus transducer size for a rectanglular and (b) F_0 versus transducer area for a cirular rectanglular.

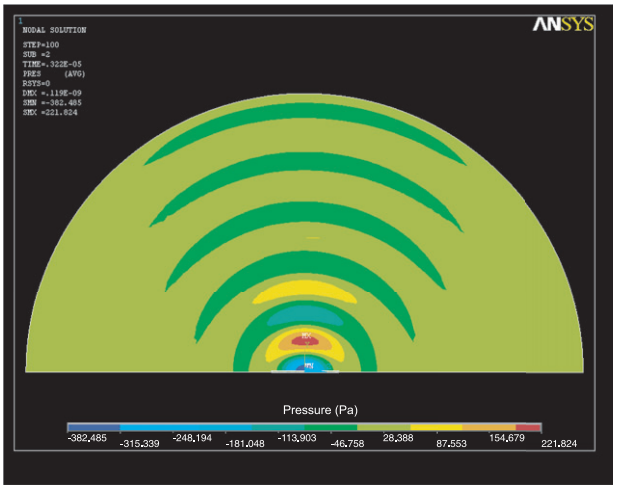

Figure 6. Pressure field above the transducer.

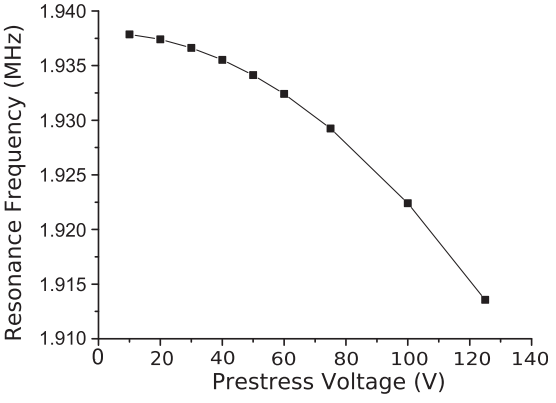

Figure 7. Resonance frequency versus prestress voltage.

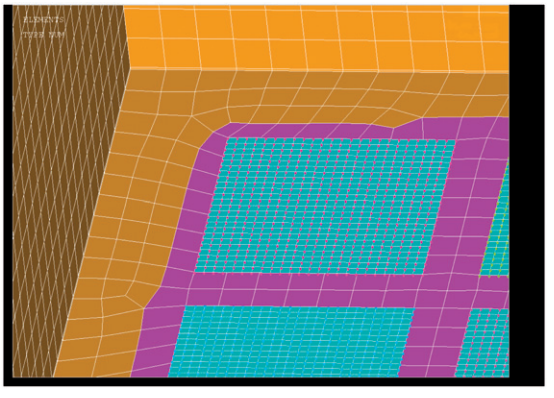

Figure 8. Array detail.

of the array. Even numbers of transducers have been used and therefore the center of the array does not coincide with a transducer.

The transducers were modelled as in the case of the single transducer. The fluid, however, was modelled differently. Instead of a hemisphere the fluid is modelled as a block since we were only interested in the focal point and consequently in the volume directly above the array. Moreover, the hemispherical model, when simulated, produced a lot of useless volume, and consequently useless elements which slow down the simulation. Furthermore, the hemisphere should be meshed with tetrahedral elements and as a consequence, a large number of elements is needed to fill a certain volume compared to hexahedral. In the case of a block we could not use *FLUID130* elements, which can only be used with spherical volumes, therefore reflections at the fluid boundaries were avoided by setting the impedance of the boundary fluid elements to 1, which resulted in full absorption of the sound waves. The different elements used are shown in Figure 8. The blue regions are the transducers and the yellow areas are the air. The purple color denotes the areas in the fluid block, where the structure-fluid coupling takes place.

Table 3. Experimental design results for a transducer array.

f_1	f_2	f_3	Pressure at focal point (Pa)
−	−	−	300
+	−	−	240
−	+	−	160
+	+	−	160
−	−	+	120
+	−	+	600
−	+	+	150
+	+	+	750

Since the CMUT array was developed for beam focusing the phases were arranged in such a way that the sound waves, produce a maximum of sound pressure at a predefined focal point through interference. The driving voltage V_{ij} of each transducer is described by the following equation:

$$V_{ij} = V_{\text{bias}} + V_{\text{amp}} * \sin(t + \Phi_{ij}) \tag{3}$$

Φ_{ij} is the phase of the transducer and it is calculated considering the position of the transducer in the array and the position of the focal point in space. By proper adjustment of the Φ_{ij} values, the waves can add constructively at the focal point located at a distance directly above the center of the array.

In order to design the phased array, the effect of different factors on the output of the array had to be determined. For this purpose we implemented a '2k factorial design'. We have initially considered five independent factors: (i) transducer size, (ii) transducer distance, (iii) number of transducers, (iv) frequency and (v) focal distance. Nevertheless, since the resonant frequency depends on the transducer size, we performed the study for the remaining three factors, keeping the transducer size constant and trying to maximize the sound pressure at the focal point.

The following factors were used:

- f_1: transducer distance, f_1 (−) 210 μm, f_1 (+) 300 μm
- f_2: focal distance, f_2 (−) 700 μm, f_2 (+) 1200 μm
- f_3: array size, f_3 (−) 2×2, f_3 (+) 6×6

and the experimental design is described in Table 3.

3.1. *Simulation results*

According to the '2k factorial design' used, the effect of each factor on the sound pressure was calculated and the results of the experimental design are shown in Table 4. As it is shown, the transducer's distance in the array has the greatest effect on pressure at focal point since the effect value is equal to 2.13, i.e. the highest among the independent factors used. On the other hand, the effect value of the focal distance is found equal to −0.08, thus the pressure exhibits weak and also negative dependance on the focal point distance.

Taking into account the effect of the transducer distance on sound pressure, we extend our study on this parameter. In particular, the pressure at focal point for a 4×4 array of

Table 4. Effect of different factors on pressure at focal point.

Factor	Effect value
Transducer distance	2.13
Focal distance	−0.08
Array size	1.58

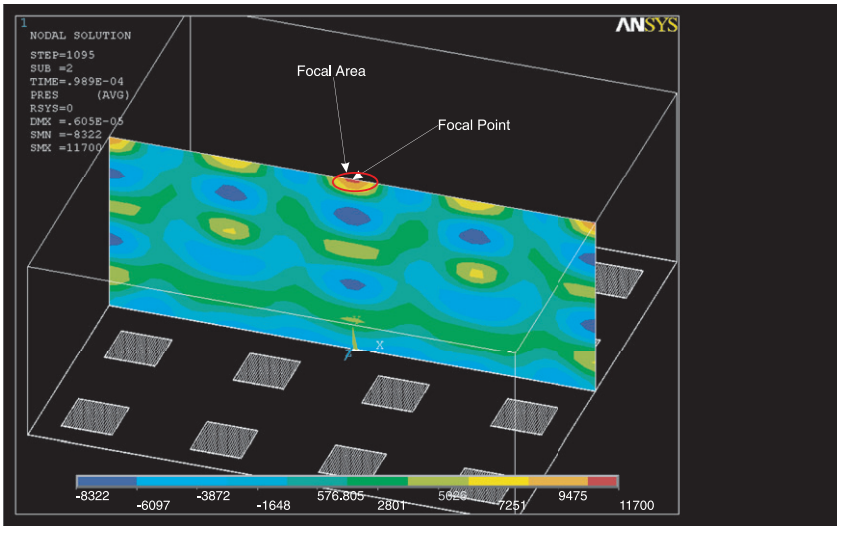

Figure 9. Pressure field at $X=0$ plane (Pa).

200 μm × 200 μm transducers was estimated for several values of the transducer distance, using time domain FEA. As it is shown in Figure 5(a) the resonance frequency of the transducers was found to be 0.691 MHz. The simulation results reveal that the maximum pressure is detected when the transducer distance is equal to 510 μm. The calculated value of the transducer lies in good agreement with previously reported work by Kazys et al. (1998), who determined analytically that maximum pressure is achieved when the transducer distance is approximately equal to 500 μm.

Figure 9 shows the architecture of the planar CMUT array and pressure field at $X=0$ plane, where the maximum pressure is denoted in red. Furthermore, the pressure at focal point as a function of time, for 6 × 6 array, is shown in Figure 10. It is characteristic that in both figures the maximum pressure exceeds 10 KPa. The ultrasound acoustic intensity thresholds for tactile sensation, was studied by Gavrilov, Tsirulnikov, and Davies (1996) and are listed in Table 5. By interpolating the P_{max} values, which where calculated using the values of acoustic intensity (Table 5), we find that when the frequency is 0.691 MHz the pressure threshold is approximately $\simeq$6810 Pa. Therefore, the maximum pressure calculated by time domain analysis (10 KPa) exceeds the pressured required for mechanoreceptor excitation. Our results for pressure are comparable with the results reported by Yamaner, Olcum, Bozkurt, Koymen, and Atalar (2010), who used an

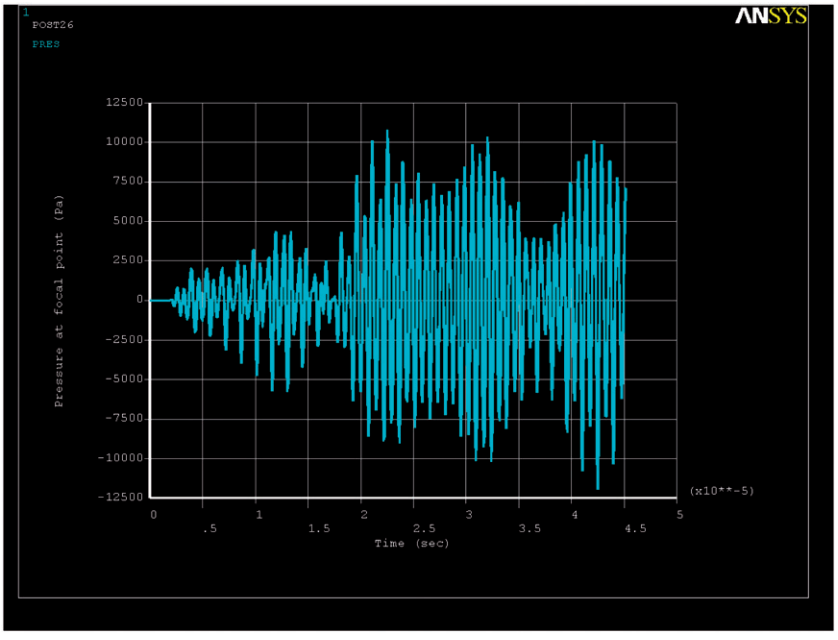

Figure 10. Pressure at focal point.

Table 5. Acoustic intensity J and pressure amplitude P_{max} threshold versus frequency.

F (MHz)	J (W/cm^2)	P_{max} (Pa)
0.480	8	5748
0.887	15	7871
1.950	80	18176
2.670	120	22262

equivalent circuit model to design high power CMUT device for ultrasound imaging. The pressure calculated in our work lies in agreement with the respective calculated by Yamaner et al.

Finally, the excitation area formed on the skin can be determined from the time domain analysis results. In particular, the size of the area with pressure above threshold (the red and yellow area above the center in Figure 9) is $\simeq$200 μm. Thus, we can conclude that since the density of the mechanoreceptors in the fingertip is 2500/cm^2, there should be at least one receptor directly underneath the excitation area.

4. Conclusion

In this article, we have demonstrated the design and FEA simulation of a CMUT-based tactile display, that uses airborne ultrasound to excite the skin mechanoreceptors and show

that a CMUT-based tactile display is feasible. Ultrasound is generated by a CMUT and a the energy is focused on the skin with the aid of a CMUT-phased array. Simulation of the individual transduce and the arrays is performed using FEA. The effect of three parameters on the pressure at focal point is studied and it was revealed that the transducer distance had the greatest effect. Furthermore, it is demonstrated that the optimal distance is 500 μm, which is in agreement with previously reported results. The pressure at focal point exceeds the required threshold for mechanoreceptor excitation and the focal area is large enough so that at least one mechanoreceptor is under the focal area. Concluding, we have shown that the design of a tactile display based on a CMUT-phased array is feasible.

Note

1. PolyMUMPS Design Handbook, Revision 11.0, Memscap Inc., Durham NC, USA.

References

Ansys Documentation (2010), Chapter 10: Mechanical APDL, Sections: 'Basic Analysis Guide' and 'Element Reference'.

Bozkurt, A. (2003), 'Finite Element Modelling of CMUTs using a Perfectly Matched Layer for Fast Simulation', in *IEEE Symposium on Ultrasonics*, 5–8 October, pp. 1979–1982.

Chouvardas, V.G., Miliou, A.N., and Hatalis, M.K. (2008), 'Tactile Displays: Overview and Recent Advances', *Displays*, 29, 185–194.

Gavrilov, L.R., Tsirulnikov, E.M., and Davies, I. (1996), 'Application of Focused Ultrasound for the Stimulation of Neural Structures', *Ultrasound in Medicine & Biology*, 22, 179–192.

Greve, D.W., and Openheim, I.J. (2003), 'Coupling of MEMS Ultrasonic Transducers', *Proceedings of IEEE Sensors*, 2, 814–819.

Hoshi, T., Takahashi, M., and Shinoda, H. (2010), 'Noncontact Tactile Display Based on Radiation Pressure of Airborne Ultrasound', *IEEE Transactions on Haptics*, 3, 155–165.

Iwamoto, T., Maeda, T., and Shinoda, H. (2001), 'Focused Ultrasound for Tactile Feeling Display', in *The Eleventh International Conference on Artificial reality and Telexistence (ICAT2001)*, pp. 121–126.

Jain, A., Greve, D.W., and Openheim, I.J. (2003), 'Experiments in Ultrasonic Flaw Detection using a MEMS Transducer', *Proceedings of SPIE*, 5057, 431–439.

Kazys R., Jakevicious L., and Mazeika L. (1998), 'Beamforming by Means of 2D Phased Ultrasonic Arrays', ISSN 1392-2114 ULTRAGARSAS, Nr.1(29), pp. 12–14.

Klein, D., Freimuth, H., Monkman, G.J., Egersdorfer, S., Meier, A., Bose, H., Baumann, M., Ermert, H., and Bruhns, O.T. (2005), 'Electrorheological Tactel Elements', *Mechatronics*, 15, 883–897.

Nakatani, M., Kajimoto, H., Kawakami, N., and Tachi, S. (2005), 'Tactile Sensation with High-density Pin-matrix', in *Proceedings of the 2nd Symposium on Applied Perception in Graphics and Visualization (APGV '05)*, ACM, New York, USA, pp. 169–169.

Saleh, K.Y., and Smith, N.B. (2004), 'Two Dimensional Ultrasound Phased Array Design for Tissue Ablation for Treatment of Benign Prostatic Hyperplasia', *International Journal of Hyperthermia*, 20, 7–31.

Teston, F., Certon, D., Patat, F., and Felix, N. (2005), 'Implementation of Master Curves for cMUT Arrays Design', in *IEEE Ultrasonics Symposium*, 18–21 September, pp. 1933–1936.

Wygant, I.O., Zhuang, X., Yeh, D.T., Nikoozadeh, A., Oralkan, O., Ergun, A.S., Karaman, M., and Khuri-Yakub, B.T. (2005), 'Integrated Ultrasonic Imaging Systems Based on CMUT Arrays: Recent Progress', in *Proceedings of the 2004 IEEE Ultrasonics Symposium*, 23–27 Augest, Vol. 1, pp. 391–394.

Yamaner, Y.F., Olcum, S., Bozkurt, A., Koymen, H., and Atalar, A. (2010), 'Optimizing CMUT Geometry for High Power', in *IEEE International Ultrasonics Symposium*, San Diego, California.